Dynamic Modeling of the Coproduction of Liquid Fuels and Electricity from a Hybrid Solar Gasifier with Various Fuel Blends

ARTICLE *in* ENERGY & FUELS · MAY 2013

Impact Factor: 2.79 · DOI: 10.1021/ef400217n

3 AUTHORS:

Ashok Athreya Kaniyal
University of Adelaide
6 PUBLICATIONS **28** CITATIONS
SEE PROFILE

Philip J. Van Eyk
University of Adelaide
27 PUBLICATIONS **145** CITATIONS
SEE PROFILE

Graham J Nathan
University of Adelaide
234 PUBLICATIONS **1,978** CITATIONS
SEE PROFILE

energy&fuels

Article

pubs.acs.org/EF

Dynamic Modeling of the Coproduction of Liquid Fuels and Electricity from a Hybrid Solar Gasifier with Various Fuel Blends

Ashok A. Kaniyal,*[,†,‡] Philip J. van Eyk,[†,§] and Graham J. Nathan[†,‡]

[†]Centre for Energy Technology, [‡]School of Mechanical Engineering, and [§]School of Chemical Engineering, The University of Adelaide, Adelaide SA 5005, Australia

ABSTRACT: A sensitivity analysis is presented of the energetic and environmental performance of a hybridized solar gasification, coal-to-liquids (CTL_{sol}) polygeneration system using a pseudo-steady-state model outlined in a recently submitted paper. The hybrid CTL_{sol} system was assumed to be integrated with pressurized (upgraded) syngas and O_2 storage to reduce the impact of solar resource transience on the unit operations downstream of the hybrid gasifier. Reported is the sensitivity of the CTL_{sol} system's energetic and environmental performance to variations in gasification reactor pressure, to turn-down in the fuel feed rate to the hybrid gasifier, to the integration of an indirectly irradiated hybrid natural gas dry or steam reforming system, and to the proportion of biomass cogasified with the coal. The energetic performance of the CTL_{sol} system was shown to be only weakly sensitive to the solar hybrid gasifier pressure. The incorporation of a natural gas steam reformer within the hybrid solar coal gasifier was shown to reduce by an additional 15% the process' mine-to-tank CO_2-e emissions relative to the configuration without the co-reformer. However, the addition of the co-reformer to the solar hybrid gasifier also reduced the solar share of the system output to 17% from 20%. The use of a dry reforming process was found to enable similar energetic and environmental performance characteristics to the steam reforming process. Mine-to-tank greenhouse gas emissions parity with diesel production from mineral sands can be achieved with a 30% biomass cogasification fraction, by weight, in a solar hybrid cogasifier, while 45 wt % biomass is required for the nonsolar equivalent. This coal-biomass solar cogasification system also achieved a 22% improvement in energetic productivity relative to the nonsolar reference system. Mine-to-tank CO_2-e emissions of 0 was found to be achievable with a biomass cogasification fraction of 60 wt %, while the nonsolar equivalent was found to require a biomass fraction of 70 wt % to enable the same outcome. Reducing the amount of biomass to achieve a given environmental target is important given that biomass is typically three to four times more expensive than coal.

1. INTRODUCTION

Synthetic liquid fuels produced by the gasification of carbonaceous fuels coupled with Fischer−Tropsch synthesis (FT) is expected to play a significant role in meeting the energy needs of the transportation sector over the next 50 years.[1] However, a barrier to the implementation of coal to Fischer−Tropsch liquid systems is that the mine-to-tank greenhouse gas (GHG) emissions are almost 2.5 times larger than those of producing diesel from tar sands and more than 6 times those of producing diesel from conventional mineral crude.[2−5] This environmental challenge offers an opportunity to identify options to reduce the CO_2-e emissions associated with producing liquid fuels by the FT process. Hence, the present assessment seeks to determine the emission reduction potential of a range of renewable energy integrated coal-to-liquid (CTL) systems.

An innovative approach to lowering the net GHG emissions of the CTL process is the introduction of concentrated solar thermal power to the endothermic, oxygen-blown, autothermal coal gasification process. The value of solar hybridization has previously received extensive treatment in the context of power generation processes.[6−9] However, the work of Kaniyal et al.[10] was the first comprehensive process analysis of a solar hybrid coal-to-liquids, CTL_{sol} polygeneration system. The pseudo-steady-state system level analysis of the CTL_{sol} system showed the potential to increase by 21% the net energy output per unit feedstock input for a full solar year and reduce by 30% the mine-to-tank greenhouse gas emissions, relative to the verified autothermal CTL_{ref} system.[10] As in other examples of solar hybrid power generation systems, the CTL_{sol} polygeneration system showed the potential to eliminate the influence of solar intermittency on unscheduled plant shut downs and, with a modest amount of syngas storage,[7−9,11] on load fluctuations in the unit operations downstream of the solar hybrid gasifier.[10] Nevertheless, the GHG emissions of the CTL_{sol} system were found to be 1.6 times larger than those associated with producing diesel from tar sands and 4 times those of producing diesel from conventional mineral crude. Thus, there is a need to identify additional approaches to further reduce CO_2-e emissions. Options to achieve this include alternative reactor operating conditions, integration of solar natural gas co-reforming processes,[12] and the cogasification of coal with biomass. Hence, the present investigation aims to assess the energetic GHG emissions and capital utilization performance impacts of each of these three options.

A significant opportunity to improve the economic and GHG emissions performance of a CTL polygeneration system was recently identified by integrating the autothermal entrained flow gasifier with a conventional tubular, pressurized steam methane reforming (SMR) reactor.[13] Blending the output from the autothermal coal gasification process, which has a low ratio of $H_2/CO \sim 0.4$, with the syngas produced by the SMR

Received: February 5, 2013
Revised: April 30, 2013
Published: May 3, 2013

   dx.doi.org/10.1021/ef400217n | *Energy Fuels* 2013, 27, 3556−3569

process, which has a high ratio of $H_2/CO \sim 3.0$, reduces the total CO_2 emissions intensity of the water−gas shift (WGS) upgrade reactions. This is because the FT synthesis process requires syngas with $H_2/CO \sim 2.26$.[3,10] Furthermore, the expected cost of integrating a tubular reformer within an entrained flow gasification system is expected to be low.[13] For the conventional gasification case, the integration of a tubular reformer was shown to increase the capital cost by <1%, offering the potential to significantly improve the viability of CTL polygeneration.[13] It should be noted, that while the total cost of this polygeneration configuration changes very little due to balance-of-plant savings, Adams and Barton[13] assume that it costs 25% more to use a radiant cooler in a gasifier with steam reforming than to use a traditional steam-only radiant syngas cooler. Furthermore, in the context of an atmospheric pressure, windowed, solar hybrid gasifier, the integration of a tubular co-reforming process offers a feasible approach to generate pressurized syngas without comprising the structural integrity of the quartz window, as would occur with the use of elevated pressures[14] and/or temperatures.[15−17] This approach could reduce the technical challenges associated with the need for a pressurized, windowed, directly irradiated, gasification, co-reforming reactor, as was recently proposed in Sudiro's study of a FT liquid polygeneration system.[12] However, to date, no assessment has been reported of the energetic and GHG emission performance of a FT liquid polygeneration system integrated with a co-reforming reactor. Hence, an additional aim of the present investigation is to meet this need.

A disadvantage of both the solar-hybridized coal gasification and the steam methane reforming process (SMR) is its large combined steam demand.[18] This is an important issue, not only because of the parasitic impact of producing steam for internal use in a polygeneration system but also because access to water is typically poor in the arid regions where the solar resource is greatest. The dry reforming of natural gas with CO_2 is one option by which the water consumption intensity of the solar-intensive portion of the CTL_{sol} polygeneration system could be reduced.[19] Such a process could also offer important synergies with CO_2 geo-sequestration pipeline networks, which are anticipated to be introduced in the medium-term.[20] Furthermore, the solar dry reforming process could also improve the viability of natural gas reserves that are currently made uneconomic by high dissolved CO_2 concentrations.[21] Hence, a further aim of the present investigation is to compare the net energetic, GHG emissions and steam consumption performance of integrating an indirectly irradiated dry co-reformer with that of a steam co-reformer within a solar hybrid coal gasification system.

The flexibility to vary the fuel feed rate to the solar hybrid gasifier in response to the amount of solar thermal power that is available has the potential to significantly improve the energetic and GHG emissions performance of the CTL_{sol} system relative to operation based on an invariant fuel feed rate.[10] One approach to increase the flexibility of the plant to respond to variations in the input of concentrated solar radiation is to allow the fuel feed rate to be boosted intermittently above the nominal design value (1 kg/s for the case investigated by Kaniyal et al.[10]). Gasifier operation with a constant fuel flow rate leads to the suboptimal use of the installed heliostat collection capacity and therefore the "spillage" of solar radiation whenever the optimal potential thermal power output of the heliostats exceeds the endothermic demand of gasifying coal at the nominal design rate of fuel flow.[10] However, the solar-boosted production of syngas has the disadvantage of increasing the polygeneration system's large, parasitic syngas compression load.[10] This is because the windowed solar-hybridized gasification process is unlikely to be feasible at elevated pressures.[22−24] One option to partially offset the solar-boosted syngas compression load is to turn-down the fuel flow rate to the hybrid gasifier below the nominal design flow rate at night, which has the added advantage of also reducing the gasifier's O_2 demand.[10] The hybrid solar gasifier and heliostat field could reasonably be expected to be the two most expensive components of a CTL_{sol} polygeneration system. This is assuming that the hybrid solar gasifier has a similar cost profile to the autothermal entrained flow gasification system[2,13,25−29] and because the heliostat field typically forms ∼50% of the cost of concentrated solar power systems.[30] Thus, the flexibility to boost and turn-down the fuel feed rate to the gasifier gives rise to an important capital productivity trade-off between the gasifier's excess thermal capacity and the installed heliostat collection capacity. No quantitative assessment of these trade-offs has been reported previously. Hence, the present investigation aims to quantify the trade-off between the performance, energy output per unit feedstock, GHG emissions, and the capital utilization of the installed excess hybrid gasifier and excess heliostat collection capacity.

Biomass cogasification is likely to be necessary to reduce the CO_2-e emissions of diesel produced by the autothermal CTL process to below that of production from conventional mineral crude or tar sands, in the absence of carbon capture and storage technology.[2,3,25,27] However, the autothermal coal-biomass-to-liquids (CTL_{bio}) process requires biomass cogasification fractions of at least 60% by weight to reduce its GHG emissions to below that of (non-tar sands/bitumen) mineral crude-derived diesel.[2,25,27] Such large cogasification fractions are likely to present significant technical challenges in both sourcing biomass at the required scale[31] and in gasifier design.[32−34] Additionally, because biomass has typically been 3−4 times more expensive than coal,[31,34−36] there are significant economic advantages in reducing the biomass fraction to achieve a given CO_2 emissions target. This could potentially be achieved by the solar-hybridized cogasification of coal-biomass since the CTL_{sol} process stores ∼23% more carbon in the FTL end product than the autothermal CTL_{ref} process.[10] However, the magnitude of these potential benefits is yet to be reported. Hence, the present investigation also aims to quantify the potential benefits of the hybridization of concentrated solar thermal radiation into the autothermal coal-biomass cogasification process for the production of FTL fuels.

The primary objective of the present assessment is to identify effective combinations of operating conditions, reactor configurations, and blend ratios of biomass with coal that achieve CO_2-e emissions parity with diesel derived from conventional mineral crude or tar sands or that achieve carbon-neutral production on a mine-to-tank basis. Specifically, the investigation aims to evaluate the operating conditions that optimize the utilization of both the hybrid gasification reactor and heliostat field. It also aims to examine the potential GHG emissions and energetic value of incorporating an indirectly irradiated, pressurized dry or steam natural gas reforming system within the solar hybrid gasifier, for the production of FTL fuels.

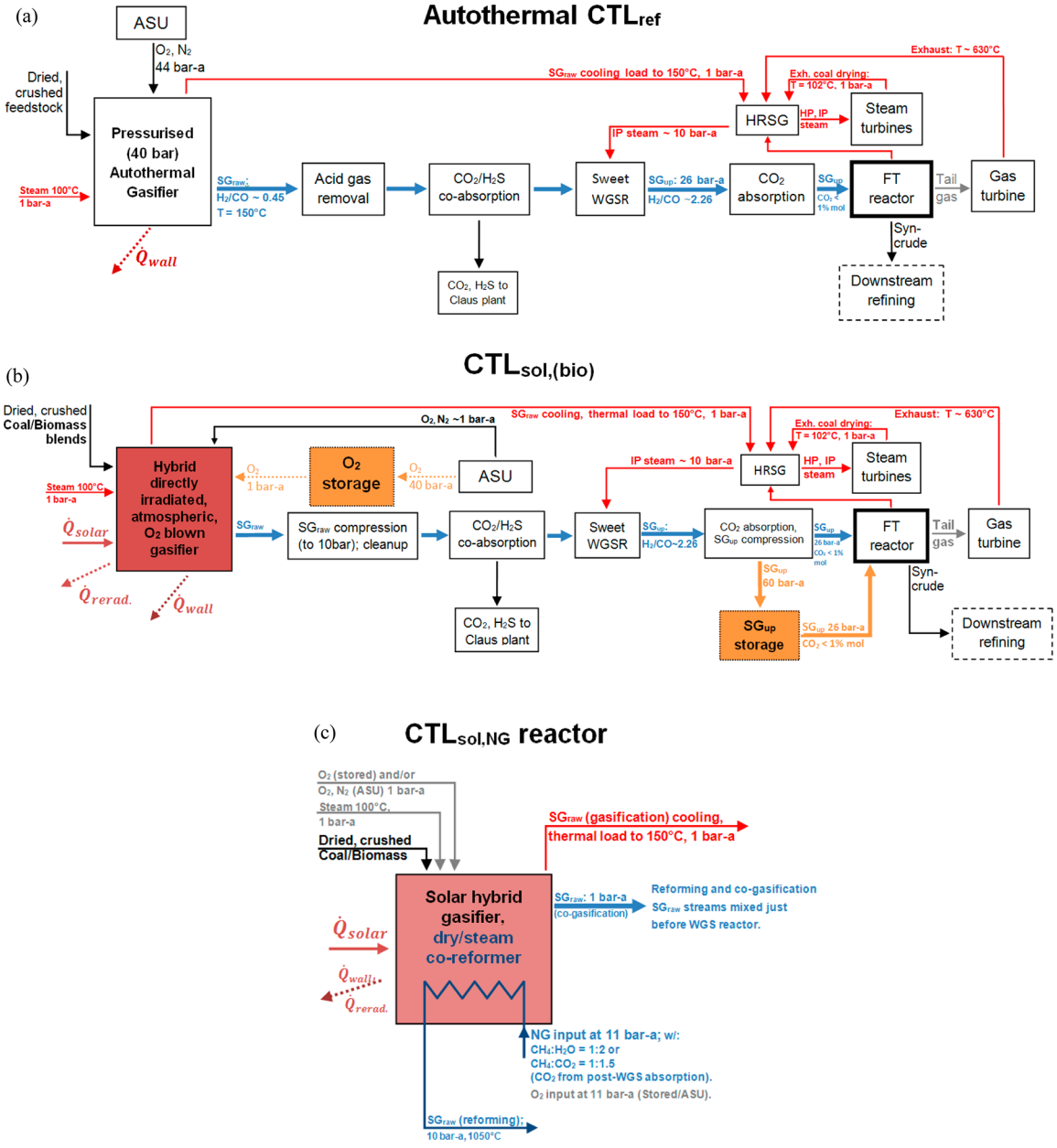

Figure 1. Simplified, annotated process schemes for the (a) reference, pressurized autothermal Shell gasification integrated CTL_{ref} polygeneration system (top); (b) CTL_{sol} polygeneration system integrated with a directly irradiated solar, O_2-blown hybrid atmospheric pressure gasifier, upgraded syngas, and O_2 storage system (middle); and (c) (c) schematic diagram of the solar hybrid gasifier/natural gas dry or steam co-reformer (bottom), which replaces the hybrid solar (co)gasifier shown in (b) and is integrated with the downstream process of the CTL_{sol} polygeneration system.

2. METHODOLOGY

The energetic and environmental performance of the solar-hybridized gasification, coal-to-liquids polygeneration system, hereafter termed CTL_{sol}, was assessed relative to a "reference" system based on a conventional, autothermal, pressurized (40 bar) "Shell"-type gasifier, hereafter termed CTL_{ref}.[3] The autothermal CTL_{ref} system developed by Kaniyal et al.[10] (see Figure 1a) is consistent with and verified against the baseline scheme investigated by Meerman et al.[3] The CTL_{sol} system was also developed and investigated by Kaniyal et al.[10] As in the authors' earlier work,[10] all scenarios investigated herein assume that all of the CO_2 produced by the facility is vented. Hence, further mitigation could be achieved were carbon sequestration to be incorporated. All unit operations, except the gasifier section, were modeled using Aspen Plus v7.1 software, while the hybrid cogasifier section of the CTL_{ref} and CTL_{sol} systems was modeled using Aspen HYSYS v7.1 software.

Figure 1 presents simplified, annotated schematic diagrams of three systems, including the baseline CTL_{sol} configuration investigated by Kaniyal et al.[10] The first additional system, shown in Figure 1b, is the $CTL_{sol,bio}$ polygeneration system used to model the solar hybrid cogasification of coal-biomass fuel blends. Figure 1c shows the second additional system, namely, the hybrid solar gasifier/co-reformer component of the $CTL_{sol,NG}$ system. This process uses a pressurized counter-current flow natural gas dry or steam co-reformer, which is integrated with the hybrid solar gasifier. A conceptual configuration of the proposed hybrid solar gasification/co-reforming reactor is shown in Figure 2, and the model is described in section 2.2.1.

Figure 2 presents the reactor configuration on which the performance calculations were based during operation with a solar input. This extends further the system proposed previously by Kaniyal et al.[10] by the addition of an indirect heat exchanger to allow the reforming of natural gas under pressure following Dahl et al.[14] Like the previous investigation, Figure 2 modifies the original solar-only

dx.doi.org/10.1021/ef400217n | Energy Fuels 2013, 27, 3556−3569

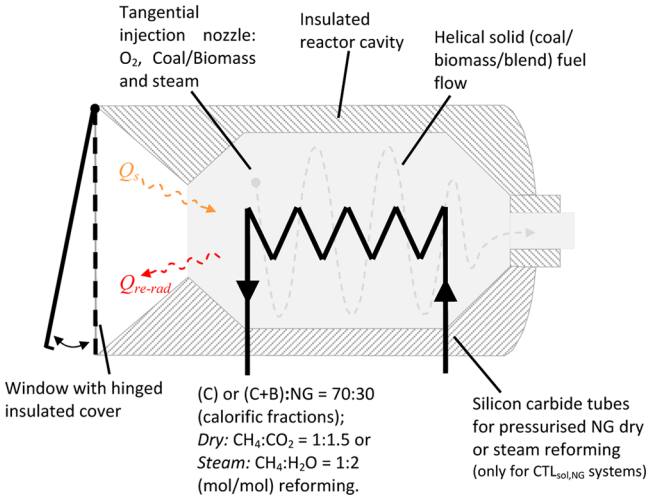

Figure 2. Configuration of the directly irradiated atmospheric pressure hybrid solar reactor used to estimate heat losses by radiation, $\dot{Q}_{rerad}$ during operation with solar thermal power input.[14] The hinged shutter is assumed to allow these losses to be avoided during autothermal gasification of coal (C) and biomass (B) blends.[10] Also shown is the configuration assumed to allow the hybrid, continuously operational co-reforming (with cogasification) of natural gas flowing counter-current to the gasification vortex stream, in pressurized, silicon carbide tubes with CO_2 as the reagent for the dry process or H_2O as the reagent for the steam reforming reactions. The indirectly irradiated, oxygen-blown natural gas reforming reactions are assumed to take place at 1050 °C and 11 bar-a.[14] The hybrid vortex gasifier and co-reforming reactor are assumed to be sized to achieve a sufficiently long residence time for 100% conversion of the coal and 99% of the input natural gas to syngas.

configuration of Z'Graggen et al.[24] by the addition of an external shutter to avoid radiant losses during periods of low solar insolation.[10]

The electricity generated by the CTL processes is designed to satisfy the parasitic demand of the various unit operations within the process. This maximizes the production of Fischer–Tropsch liquid fuels (FTL), minimizes the number of energy processing steps between the feedstock and final energy product, and avoids any diversion of the upgraded syngas to the gas turbine for electricity generation. The upgraded syngas, SG_{up}, is produced in the sweet water–gas shift reactor, SWGSR, to achieve a composition with H_2/CO (mol/mol) ~ 2.26[3] as is required for the Fischer–Tropsch reactor (FTR). Relative to the heating value of the coal input, the parasitic electrical output is ~15% for all scenarios. Avoiding exporting electricity is likely to be the best option at the small scale considered here because the additional investments in substation and electricity transmission infrastructure are likely to be considerable. However, there may be scenarios in which it could be desirable to configure a plant to also supply peaking power during periods of high electricity prices.

The sensitivity of the energetic and environmental performance of the CTL_{sol} polygeneration system proposed by Kaniyal et al.[10] is assessed for variation of the following parameters:

- the pressure of the gasifier reactor over the range of 1 to 4 bar-a
- the feed rate of fuel to the hybrid gasifier in response to the transient availability of solar radiation, for four heliostat collector area scenarios (A_{coll}); see Table 4
- the type of natural gas reforming (NGR): dry (CO_2) or steam methane reforming (SMR);
- the biomass (B) weight fraction relative to that of coal (C) in the fuel blend (m_B/m_{C+B}): {0, 10, 20, 30, 60, and 100%}.

2.1. Solar Resource Analysis. The study year selected for all simulations of the CTL_{sol} system is the summer-to-summer period: 1 Jun 2004 to 31 May 2005. The insolation data set corresponded to the Farmington site in northern New Mexico (USAF #723658) whose latitude is 37°N (USAF #723658).[37,38] The net solar thermal power input to the hybrid solar gasifier ($\dot{Q}_{sol,net}$) was estimated using eq 1. In eq 1, $\dot{Q}_{wall}$ is the assumed rate of heat lost through the gasifier walls and η_{opt} is the optical efficiency of all mirrors and reflectors, including the compound parabolic concentrator, which was assumed to be 50%.[10] The hourly averaged rate of reradiation losses through the quartz window was calculated using the solar absorption efficiency parameter, η_{abs}. This parameter was calculated using eq 2 for each gasification temperature (T_g), which spanned the range of 1100–1400 °C. For the year-long solar insolation time series, η_{abs} was calculated for each hour assuming a mean solar flux concentration ratio ($\tilde{C}$) of 2000 suns[39] and a reactor design with an optimal aperture size that maximises the capture of radiation from the heliostat field and minimises radiation losses from the aperture.[17] The hybrid solar gasifier was also assumed to lose heat through the reactor walls at a rate equal to $\dot{Q}_{wall}$, which is given by eq 3.[40] Figure 3 presents the relationship between η_{abs} and solar insolation (I)[17] for four gasification reactor temperatures.

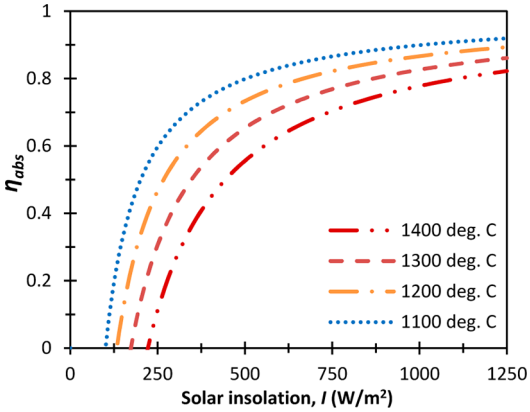

Figure 3. Dependence of solar absorption efficiency (η_{abs}) on the direct normalized solar radiation intensity for T_g: 1100–1400 °C and for $\tilde{C}$ = 2000 suns.[17]

Using the solar insolation time series data set, a time series for $\dot{Q}_{sol,net}$ was calculated for a given heliostat collection area (A_{coll}) and gasification temperature (T_g). The parameter $\dot{Q}_{sol,net}$ is normalized by $\dot{Q}_{HG\text{-}(NGR)}^{T_g\text{-}R}$, the power required by the hybrid gasifier and natural gas reformer (under the conditions shown in Table 2) to obtain the dimensionless parameter, Φ, shown in eq 4.

$$\dot{Q}_{sol,net} = \eta_{abs}\eta_{opt}A_{coll}I - \dot{Q}_{wall} \quad (1)$$

$$\eta_{abs} = 1 - \left(\frac{\sigma T_g^{\,4}}{I\tilde{C}}\right) \quad (2)$$

$$\dot{Q}_{wall} = \dot{m}_{coal} \times 0.03 \times Q_{coal(HHV)} \quad (3)$$

$$\Phi = \frac{\dot{Q}_{sol,net}}{\dot{Q}_{HG\text{-}(NGR)}^{T_g\text{-}R}} \quad (4)$$

2.2. Pseudodynamic Process Model. The simulation of the CTL_{sol} process model in the present investigation is based on the pseudodynamic model detailed previously.[10] Following that work, all scenarios assessed herein were optimized to maximize the production of Fischer–Tropsch liquids. The dynamic operation of the CTL_{sol} system was modeled using an in-house MATLAB code that employed a steady-state approximation for each time-step, based on simulations in Aspen Plus and Aspen HYSYS (v 7.1). The MATLAB code used unique linear or log–linear relationships to describe the parasitic load, energetic output, and CO_2 emissions of each unit operation of the CTL_{sol} polygeneration system for each scenario summarized in section

dx.doi.org/10.1021/ef400217n | Energy Fuels 2013, 27, 3556–3569

2.1. The part-load performance of each unit operation was accounted for by following the methodology outlined previously.[10] The unique components of all of the CTL_{sol} systems, in comparison with the CTL_{ref}, namely, the SG_{up} storage system and the O_2 storage system, are illustrated in the process model of Figure 1(b).

For all of the scenarios modeled herein, the capacity of the upgraded syngas (SG_{up}) storage tank was assumed to be equal to 8 h of SG_{up} output from the water−gas shift reactor at a rate corresponding to operation of the hybrid solar gasifier at 1100 °C, 1 bar-a, and $\Phi = 0$. The sensitivity of this assumption of energetic performance was assessed by Kaniyal et al.[10] for three cases of storage tank capacity, equal to 4, 8, and 16 h of SGup production, at the hourly rate specified in the previous sentence. This analysis showed that the main effect of increased storage capacity on the energetic and environmental performance of the CTL_{sol} system was on the statistical variance in SG_{up} throughput to the FTR, which was assumed to have good part-load performance down to 40% of its rated capacity.[3]

Oxygen produced in the air separation unit (ASU) was assumed to be stored in a pressurized tank at 60 bar-a. A fixed O_2 storage capacity of 5000 kmol (at 94.3% mol ∼ 3300 m^3) was assumed for all cases. This was based on the finding of Kaniyal et al.[10] that the hybrid system's energetic and greenhouse gas (GHG) performance is only weakly sensitive to the capacity of O_2 storage.

2.2.1. Hybrid Solar Autothermal Gasifier Sensitivity to Operating Conditions. Reactor Pressure. The solar hybrid coal gasification reactor was also modeled using the same methodology and the boundary conditions as Kaniyal et al.[10] The impact of increasing reactor pressure from 1 to 4 bar-a was assessed for gasifier reactor temperatures (T_g) of 1100 and 1400 °C. Although technical feasibility of the windowed, solar hybrid gasification reactor under pressurized conditions is not yet verified, the objective of the present analysis is to assess the magnitude of any potential benefits from pressurized operation.

Fuel Flow Flexibility. The present model allows the solid fuel flow rate to the hybrid gasifier to be varied in response to variations in the solar flux from a heliostat field of a given area (A_{coll}). This differs from the earlier work,[10] which assumed a constant coal (C) flow rate of 1 kg/s ($\dot{m}_C$) to the gasifier and varied the rate of O_2 and steam flow rate to the gasifier as a function of the solar thermal power input ($\dot{Q}_{sol,net}$). The earlier assumption of a fixed fuel flow rate to the gasifier places an upper limit on the amount of solar energy that can be absorbed of $\dot{Q}_{HG\text{-}(NGR)}^{T_g\text{-}R}$. This corresponds to the amount of solar thermal power required by the hybrid gasifier to completely gasify 1 kg/s of coal or a coal-biomass blend fed to the reactor, operating at temperature T_g. Hence, when $\dot{Q}_{sol,net} > \dot{Q}_{HG}^{T_g\text{-}R}$ for a heliostat field of a given capacity, solar thermal power is spilled at the rate $\dot{Q}_{sol,net} - \dot{Q}_{HG}^{T_g\text{-}R}$. Here, the spillage of solar energy can be reduced (or even avoided) if the gasifier is operated with the flexibility to increase the fuel flow rate above 1 kg/s, on a pro rata basis when $\dot{Q}_{sol,net} \geq \dot{Q}_{HG}^{T_g\text{-}R}$. This flexibility has two advantages. First, it enables the solar share of the syngas produced to be increased, thereby improving energetic productivity and GHG emissions, and second, it enables greater economic utilization of the installed heliostat collection capacity. In addition, it reduces $\dot{m}_{C+B}$ from a reference flow rate of 1 kg/s at night, offering the potential to improve plant productivity by reducing both the gasifier's O_2 demand and also the larger, solar-boosted SG compression load during the day when $\dot{m}_{C+B}$ is increased above 1 kg/s.

The size of the energetic and GHG emissions performance improvements possible is limited by the gasifier's turn-down and turn-up capacity. Here it is assumed that the maximum and minimum limits of turn-down are ±20% from the reference flow rate of $\dot{m}_{C+B} = 1$ kg/s. The four coal(+biomass) fuel flow rate flexibility scenarios are summarized in eq 5.

$$\dot{m}_{C+B(max,min)} = \dot{m}_{(1.2,0.8)}\ \text{kg/s};\quad \dot{m}_{(1.2,0.9)}\ \text{kg/s};\quad \dot{m}_{(1.1,0.8)}\ \text{kg/s or}\quad \dot{m}_{(1.1,0.9)}\ \text{kg/s} \tag{5}$$

Capital Utilization Analysis. The capital utilization analyses were limited to the hybrid solar entrained flow gasifier and heliostat collectors (see section 2.3), given their large expected proportional contribution to the total plant cost. This assumption is based on the solar hybrid gasifier having a similar cost profile to the nonsolar, autothermal entrained flow gasifier, which forms the single largest cost component of a CTL polygeneration system[2,13,25−29] and because the heliostat collectors typically contribute 50% of the capital outlay of CSP plants.[30] Here, it is important to note that a complete assessment of the economic viability of the CTL_{sol} polygeneration system has not been carried out as it is outside of the scope of the present assessment.

The annually averaged utilization of the hybrid gasifier was calculated using eq 6 based on its maximum fuel flow rate capacity. This equation defines the annually averaged utilization as the mean of the hourly averaged flow of the coal or coal-biomass (C+B) fuel blend to the hybrid gasifier as a ratio of the maximum fuel flow rate capacity.

$$\overline{U_{HG}} = \overline{\left(\frac{\dot{m}_{C+B,hr}}{\dot{m}_{C+B(max)}}\right)} \tag{6}$$

2.2.2. Integration of an Indirectly Irradiated Pressurized, Natural Gas (Dry/Steam) Reformer. Figure 1c presents a schematic diagram of $CTL_{sol,NG}$ polygeneration system, which was modeled with a 30:70 calorific ratio of natural gas (NG) to solid fuels (coal and biomass). As shown in Figure 1c, the raw syngas output from the steam or dry reforming process was assumed to be cooled in the HRSG and then combined with the (co)gasification raw syngas output stream after it is cleaned just before the sweet WGS reactor. The combined syngas stream was assumed to be upgraded in the WGS reactor to a H_2/CO ratio of 2.26 by varying the steam flow to the reactor depending on the H_2/CO ratio of the combined syngas input. The system was assessed for both coal alone and for a coal-biomass blend with $m_B/m_{C+B} = 0.3$ (see Figures 17 and 18). The assumed natural gas composition is given in Table 1, and the operating conditions are summarized in Table 2.

Table 1. Assumed Composition and Higher Heating Value of Natural Gas (NG)

component	mole fraction
CH_4	95.2%
C_2H_6	2.5%
C_4H_8	0.3%
N_2	1.3%
CO_2	0.7%
HHV (MJ/kg)	53.2

The calculation of the parameters in Table 2 is based on the assumptions outlined below. All scenarios modeled assume that the NG flow rate is fixed, while the solid fuel flow rate is varied in response to the amount of solar thermal power that is available, as summarized by eq 5. This assumption was made because the indirect reforming process has a lower heat transfer efficiency than the directly irradiated gasification process.

Figure 2 shows a configuration of the solar hybrid reactor, with an integrated tubular silicon carbide reformer. The tubular reforming reactor was assumed to operate at 11 bar-a, while the supply pressure of natural gas was assumed to be 30 bar-a.[13] The model assumes that the reactor can be developed to achieve equilibrium conversion of the natural gas under the heat duties and syngas outlet performance conditions summarized in Table 2, so neither depends on, nor accounts for, the details of the configuration shown in Figure 2. Nevertheless, the reformer is likely to be most effective in driving the endothermic reforming reactions to completion if the flow of natural gas and the reforming reagent in the pressurized tubes is counter-current to the gasification vortex stream and to the incoming radiation. This configuration leads to the highest flux of solar energy being at the outlet end of the reformer. When 99% conversion of the fuel is assumed, the model also implicitly assumes that the combined assembly can be made large enough and/or incorporate sufficient swirl to achieve enough residence time for this to occur. Furthermore, it is worth noting that unlike the natural gas reformed integrated within the radiant cooler section of the entrained flow gasifier proposed by

dx.doi.org/10.1021/ef400217n | Energy Fuels 2013, 27, 3556−3569

Table 2. Model Input Parameters for the Solar-Hybridized, Indirectly Irradiated, Tubular, Pressurized, Natural Gas (NG) Dry and Steam Reforming Reactor Configurations

parameter		units	value				
operating pressure		bar-a	11				
operating temperature		°C	1050				
natural gas flow rate ($\dot{m}_{NG}$)		kg/s	0.20				
steam reforming	H_2O (340 °C, 11 bar-a)	kg/s	0.40				
dry reforming	CO_2 (98.3% mol)	kg/s	0.73				
ratio of net solar thermal power input to power required by natural gas reformer	Φ_{NGR}	%	0	25	50	75	100
steam reforming	thermal power load ($Q_{sol,net-NGR}$)	MW_{th}	0	1.3	2.6	3.9	5.2
dry reforming			0	1.2	2.3	3.5	4.7
steam reforming	oxidant (O_2 at 94.3 mol %)	kg/s	0.32	0.24	0.16	0.08	0
dry reforming			0.29	0.22	0.14	0.07	0

Adams and Barton,[13] in the present solar reactor, the particles are assumed to flow in a vortex around the outside of the reactor, radiating heat to the natural gas reforming tubes. Hence, the present model implicitly assumes that any potential influences of slagging and fouling of the tubes can be remedied.

Reradiation losses from the hybrid gasifier−reformer system as a whole are accounted for separately by the methodology detailed by Kaniyal et al.[10] (also summarized in section 2.1). The integration of the hybrid, indirectly irradiated, oxygen-blown, tubular reformer was assumed not to impact on the vortex reactor's reradiation characteristics and thus its absorption efficiency.[10] While the complete system is yet to be demonstrated, sufficient information is available on the performance of all components as stand-alone items to enable the performance to be estimated with the assumption that the components are all independent.

Table 2 summarizes the modeling parameters that were used to simulate the solar hybrid co-reforming system. Following Melchior et al.,[41] it was assumed that approximately 15% of the heat delivered to the reforming tubes is lost by conduction through the walls of the tubular reactor. This loss to the surroundings is used to calculate the net thermal power required by the tubular reforming reactor ($\dot{Q}_{sol,net-NGR}$), given in Table 2, to convert >99% of the methane in the natural gas to raw syngas (see Figure 2). The O_2 flow rate to the tubular reformer was assumed to be varied in response to the solar thermal power input to the reactor, to maintain a constant raw syngas output temperature of 1050 °C. Specifically, the oxidant feed to the reforming reactor is varied between 0.32 and 0 kg/s for the steam co-reforming scenario and 0.29 and 0 kg/s for the dry co-reforming process (Table 2). This is consistent with the steam reforming reaction having a slightly lower reaction enthalpy than the dry reforming process, as is apparent from reactions 7 and 8. Both the dry and steam reforming reactions were modeled using the Gibbs minimization reactor in Aspen Plus.

The proposed hybrid solar gasification, co-reforming system is assumed to operate continuously with constant flow rates both of natural gas and either one of the two reforming reagents, CO_2 or H_2O. To minimize carbon deposition, the dry reforming reactor was modeled with a CH_4/CO_2 molar ratio of 1:1.5[20] and the steam reforming model with an input CH_4/H_2O molar ratio of 1:2.[18] The CO_2 demand of the natural gas dry reforming process was assumed to be met by the post-WGS capture of CO_2 (see Figure 1c). The consumption of CO_2 by the reforming process is accounted for in the process' lifecycle emissions analysis. The CO_2 that is not consumed by the reforming process, typically 55−70% of the plant's total CO_2 emissions, is assumed to be vented to the atmosphere. Further mitigation of CO_2 is thus possible either by reuse or sequestration of this stream.

$$CH_4 + CO_2 \rightarrow 2CO + 2H_2 \quad \Delta H^{\circ}_{298K} = +247\ \text{kJ/mol} \tag{7}$$

$$CH_4 + H_2O \rightarrow CO + 3H_2 \quad \Delta H^{\circ}_{298K} = +206\ \text{kJ/mol} \tag{8}$$

Table 3. Assumed Proximate and Ultimate Analysis of Cane Trash[42] and Illinois #6 Coal[3,10]

proximate analysis (%)	biomass (B)	Illinois #6 coal (C)
moisture (AR)	35	11.1
ash (dry)	12	10.9
HHV (dry) (MJ/kg)	19.5	30.5
volatile matter (d.a.f.)	83	44.2
fixed carbon (d.a.f.)	17	55.8
ultimate analysis (% d.a.f.)		
carbon	45	80.5
hydrogen	5.8	5.7
oxygen	44	8.7
nitrogen	0.6	1.6
sulfur	0.2	3.2

2.2.3. Hybrid Solar Cogasification of Coal-Biomass Blend. Table 3 presents the proximate and ultimate analyses of both the cane trash,[42] the design biomass feedstock, and the Illinois #6 coal.[3] These two fuels are assumed to be blended at biomass weight fractions (m_B/m_{C+B}) of 10, 20, 30, 60, and 100%. All coal-biomass cogasification scenarios investigated here are identified by the symbol $CTL_{sol,bio\text{-}X\%wt}$, where X = ($m_B/m_{C+B}$). The assessment of carbon emissions also assumed the biomass to be 100% renewable and thus ignored the extraneous emissions associated with fuel harvest and transport.

The solar hybrid cogasification model assumes that the fuel blend is dried to <2 wt % moisture by the atmospheric pressure exhaust from the low-pressure steam turbine prior to being fed into the gasifier. Following Kaniyal et al.,[10] the hybrid cogasification simulation assumes that the O_2 and steam flow rate to the cogasifier is varied to maintain a constant gasification temperature of 1100 °C and char conversion of 100%.[10] The coal-biomass hybrid solar cogasification model further assumes that the fuel flow rate can be varied in response to the amount of solar thermal power available through any given hour as described in section 2.2.2.

2.3. Mine-to-Tank (MTT) CO_2-e Emissions. The greenhouse gas emissions calculated for all scenarios account for all of the emissions associated with the predicted energy output bar of the CO_2-e emissions associated with fuel combustion at the point of end-use. The emission sources accounted for herein are those from mining the coal resource, producing FT liquid fuels by the fuel-to-liquid polygeneration process, and refining the synthetic fuel[4] to diesel and all miscellaneous transportation emissions.[4] The CO_2-e emissions calculated for the cogasification scenarios assume biomass to be carbon-neutral.[2,3,25,27] Furthermore, for these scenarios, the MTT CO_2-e emissions are credited for the molar proportion of biomass combusted at the point of end-use. In addition, the emissions associated with building the solar plant are not accounted for in the present analysis, given its small contribution over the life of the facility. It should also be noted that use of the CO_2 physical absorption system provides an industrially pure stream of CO_2 which, if sequestered,

dx.doi.org/10.1021/ef400217n | Energy Fuels 2013, 27, 3556−3569

would further reduce the net CO_2 emissions from the baseline CTL_{sol} process by approximately 50%.

2.4. Heliostat Field Size Area Sensitivity. The impact of the heliostat field area (A_{coll}) on the energetic productivity and CO_2-e emission performance of the hybrid solar polygeneration system is assessed for four A_{coll} scenarios over the range of 33×10^3 to 89×10^3 m^2. Following the work of Kaniyal et al.,[10] each A_{coll} scenario is normalized using eq 9 as $\Phi_{peak}^{A_{coll}}$. Here, $\Phi_{peak}^{A_{coll}}$ is the fraction by which the annual, peak hourly averaged thermal power output of a heliostat field of a given collection capacity, $(\dot{Q}_{sol,net}^{A_{coll}})_{ann(peak)}$, exceeds the endothermic demand of the hybrid solar gasification reactor and natural gas reformer, $\dot{Q}_{HG\text{-}(NGR)}^{T_g\text{-}R}$ (for the relevant scenarios). The A_{coll} scenarios and the corresponding normalized parameters are summarized for the CTL_{sol} plant configuration and the two $CTL_{sol,NG}$ configurations in Table 4.

$$\Phi_{peak}^{A_{coll}} = \frac{(\dot{Q}_{sol,net}^{A_{coll}})_{ann(peak)}}{\dot{Q}_{HG\text{-}(NGR)}^{T_g\text{-}R}} \quad (9)$$

Table 4. Relationship between the Heliostat Field Collector Area (A_{coll}) and $\Phi_{peak}^{A_{coll}} - 1$

scenario	CTL_{sol}[a]	$CTL_{sol,NG}$ (dry)[a]	$CTL_{sol,NG}$ (steam)[a]
coal fuel flexibility scenario and NG fuel flow (kg/s)	$\dot{m}_{C(min,max)}$ = (1.2,0.8)	$\dot{m}_{C(min,max),NG}$ = ((1.2,0.8),0.2)	
gasifier maximum thermal capacity (MW_{th} − HHV)	34	34	
co-reformer maximum thermal capacity (MW_{th} − HHV)	0	10	
A_{coll} ($\times 10^3$ m^2)		$\Phi_{peak}^{A_{coll}} - 1$	
89	not assessed	1.41	1.49
63	1.39	0.72	0.78
51	0.91	0.38	0.42
44	0.68	0.21	0.25
38	0.44	not assessed	not assessed

[a]For the CTL_{sol} scenario hybrid gasifier assumed to operate at 1100 °C and 1 bar-a; for $CTL_{sol,NG}$, see Table 3.

2.4.1. Capital Utilization Analysis. The second component of the capital utilization analysis is that of the heliostat collector field. This is assumed to be the other most significant capital expense on the basis that numerous assessments of concentrated solar electrical power systems have shown that the cost of the heliostat field contributes ~50% of the total capital expense.[30] Equation 10 is used to estimate the hourly averaged utilization of the installed heliostat collection capacity as the ratio of the amount of solar thermal power consumed by the hybrid solar gasifier and co-reforming system (if applicable) to the output of the heliostat array for that hour—calculated using eq 1. In eq 10, $\dot{Q}_{HG\text{-}(NGR)}^{T_g\text{-}R}$ is the combined endothermic load of the hybrid solar gasifier operating with a coal or a coal-biomass (C+B) blend, fuel flow rate of 1 kg/s, and (if applicable) the natural gas reformer whose operating conditions are outlined in Table 2. The annually averaged utilization of the heliostat field was calculated by taking the mean of the $U_{A_{coll},h}$ time series.

$$U_{A_{coll},h} = \begin{cases} 1; & \text{if } \dot{Q}_{sol,net,h} \le \dot{Q}_{HG\text{-}(NGR)}^{T_g\text{-}R} \\ \left(\dfrac{\left(\dot{m}_{C+B} \times \dot{Q}_{HG}^{T_g\text{-}R} \right)_h}{\dot{Q}_{sol,net,h}} \right); & \text{if } \dot{Q}_{sol,net,h} > \dot{Q}_{HG\text{-}(NGR)}^{T_g\text{-}R} \end{cases} \quad (10)$$

3. RESULTS

3.1. Hybrid Solar CTL System (CTL_{sol}). *3.1.1. Reactor Pressure.* Figures 4 and 5 present the dependence on the gasification reactor pressure of the CTL_{sol} system's specific net electrical (W_{net}/Q_{coal}) and FTL (Q_{FTL}/Q_{coal}) output. Figure 4 shows that W_{net}/Q_{coal} is increased by 21% (at 1100 °C) and 29% (at 1400 °C) for an increase in gasifier pressure from 1 to 4 bar-a. In contrast, Figure 5 shows the CTL_{sol} system's FTL productivity to be fairly insensitive to gasification pressure for both gasification temperatures presented. Indeed, the difference between the maximum and minimum Q_{FTL}/Q_{coal} or both curves was calculated to be less than 1% across the temperature range of 1100−1400 °C. Further, it is important to note that Q_{FTL}/Q_{coal} is 6−8 times larger than W_{net}/Q_{coal} for all reactor pressure and temperature scenarios. Hence, the overall energetic performance of the CTL_{sol} polygeneration system is largely insensitive to gasifier pressure. This is an important result given the significant technical challenges associated with the feasible operation of a windowed solar vortex reactor at elevated pressures and temperatures >1100 °C.[15−17]

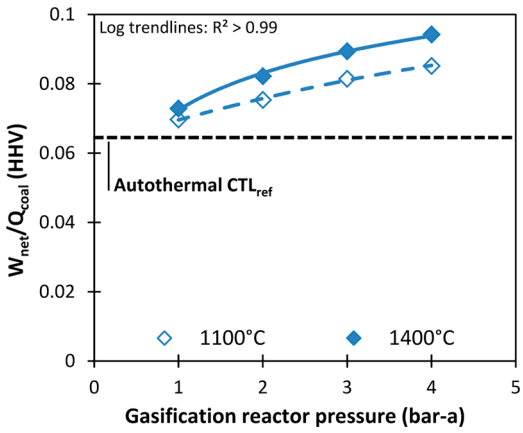

Figure 4. Dependence on the gasification pressure (bar-a) of the CTL_{sol} system's net electrical output normalized by the coal input on a higher heating value basis, for T_g = 1100 and 1400 °C. Assumptions: A_{coll} = 63×10^3 m^2, $\dot{m}_{(1.2,0.8)}$ kg/s coal flow flexibility operational scenario.

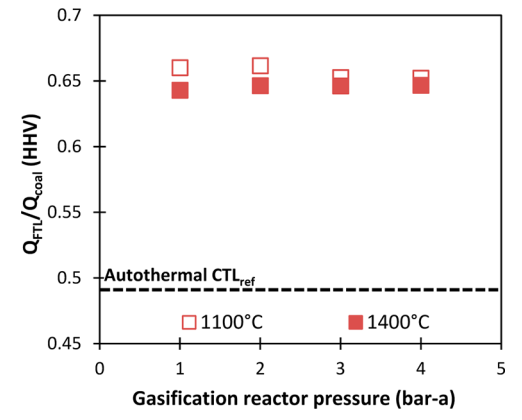

Figure 5. Dependence on the gasification pressure (bar-a) of the CTL_{sol} system's FTL production normalized by the coal input on a higher heating value basis, for T_g = 1100 and 1400 °C. Assumptions: A_{coll} = 63×10^3 m^2, $\dot{m}_{(1.2,0.8)}$ kg/s coal flow flexibility operational scenario.

dx.doi.org/10.1021/ef400217n | Energy Fuels 2013, 27, 3556−3569

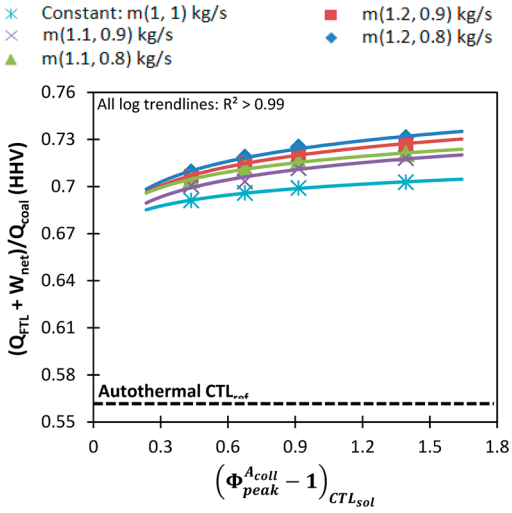

Figure 6. Dependence of the CTL_{sol} system's total energetic productivity on the normalized representation of the excess heliostat collection capacity, for four operational flexibility scenarios denoted in terms of the $\dot{m}_{(max,min)}$ kg/s limit on the fuel flow rate to the hybrid gasifier. Assumptions: T_g = 1100 °C and P_g = 1 bar-a.

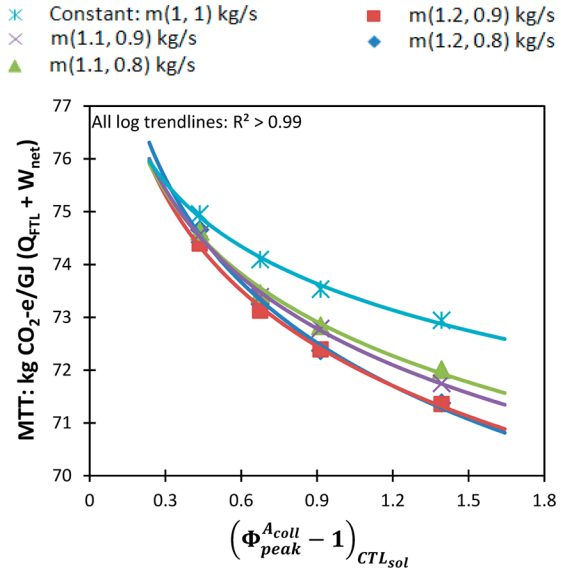

Figure 7. Dependence of the CTL_{sol} system's mine-to-tank (MTT) GHG emissions on the normalized representation of the excess heliostat collection capacity, for four operational flexibility scenarios denoted by the $\dot{m}_{(max,min)}$ kg/s limit on the fuel flow rate to the hybrid gasifier. Assumptions: T_g = 1100 °C and P_g = 1 bar-a.

3.1.2. Fuel Flow Flexibility. Figure 6 presents the dependence of the CTL_{sol} system's specific total energetic productivity $-(W_{net} + Q_{coal})/Q_{coal}$ on the normalized heliostat collection capacity, $\Phi^{A_{coll}}_{peak} - 1$, for five cases of fuel boost/turn-down, that is, $\dot{m}_{(max,min)}$. In all cases, the total productivity increases with heliostat collection area, as expected. However, the dependence on $\Phi^{A_{coll}}_{peak} - 1$ is relatively weak, so that increasing it by a factor of 3.2 increases the energetic productivity by ~2−3% relative to the autothermal CTL_{ref} system. Significantly, a greater benefit is achieved by introducing a flexible flow rate, with the $\dot{m}_{(1.2,0.8)}$ kg/s coal flow flexibility scenario estimated to improve the CTL_{sol} system's specific, total energetic productivity by 25−29% relative to the CTL_{ref} autothermal polygeneration system. This constitutes an improvement of 3−5 percentage points over the estimated improvement in energetic productivity for the constant flow rate CTL_{sol} operational scenario (for $0.44 < \Phi^{A_{coll}}_{peak} - 1 < 1.39$). The improvement in energetic output for the $\dot{m}_{(1.1,0.9)}$ kg/s operational flexibility scenario is 23−26% relative to the CTL_{ref} system over the range of A_{coll} scenarios studied. Given the heliostat field has a high capital cost, the capacity to control the fuel input to the hybrid gasifier could deliver a significant economic benefit.

Figure 7 presents the dependence of the CTL_{sol} system's mine-to-tank CO_2-e emissions on $\Phi^{A_{coll}}_{peak} - 1$ for the same set of scenarios as Figure 6. For this case, the dependence on A_{coll} is greater than that on turn-down over these ranges. Relative to the constant flow rate scenario, the $\dot{m}_{(1.2,0.8)}$ and $\dot{m}_{(1.2,0.9)}$ kg/s coal flow flexibility scenarios are predicted to enable a modest 2% reduction in emissions for $A_{coll} = 63 \times 10^3$ m^2. Consistent with Kaniyal et al.,[10] tank-to-wheel emissions were found to not vary appreciably from 63 kg CO_2-e/GJ ($Q_{FTL} + W_{net}$) for the set of operational scenarios examined here. It is thus apparent that the benefit of operational flexibility in the fuel feed rate to the hybrid gasifier is largely to improve the productivity of the CTL_{sol} system's energetic output rather than influence its GHG emissions performance. Also, as expected, there is a benefit to energetic productivity of turning up the fuel flow rate to the gasifier, and hence to having a hybrid gasifier with a larger thermal throughput capacity with excess heliostat collection capacity.

Capital Utilization Analysis. Figure 8 presents the normalized probability distribution of the hourly averaged utilization of the $U_{A_{coll},h}$ of the installed heliostat capacity for three coal flow rate flexibility scenarios. These probabilities were calculated only for the cases when the solar input to the reactor exceeds the reradiation losses, that is, when $\eta_{abs} > 0$, to avoid the large nocturnal peak that would otherwise dominate the distribution. It also combines the cases with different minimum mass flow rates into one curve since only the maximum limit on the range of fuel flow rate flexibility was found to influence the utilization of the heliostat field. This figure shows that the highest peak in the distribution corresponds to full utilization of the installed heliostat

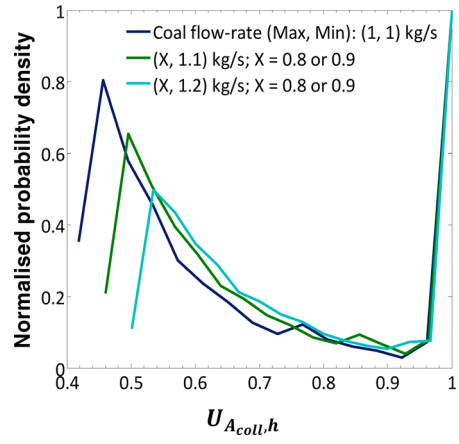

Figure 8. Normalized probability density distribution of the hourly averaged utilization of the installed heliostat collection capacity for three coal flow rate scenarios. These distributions are presented only for positive solar inputs to avoid the large nocturnal peak for clarity. Assumptions: $A_{coll} = 63 \times 10^3$ m^2, gasification at 1100 °C and 1 bar-a.

dx.doi.org/10.1021/ef400217n | Energy Fuels 2013, 27, 3556−3569

collection capacity (i.e., $U_{A_{coll},h} = 1$). These periods of full utilization occur when $\Phi \leq 1$ and can largely be attributed to solar hours in winter and at dusk/dawn when insolation is inherently low. However, the area under this part of the curve is low relative to the more significant peak in the distribution when $U_{A_{coll},h}$ is between 46 and 54%. This more significant peak corresponds to periods of seasonally high solar insolation when the maximum solar output of the heliostat field is approximately double the hybrid gasifier's endothermic demand. Here, operation of the hybrid gasifier with the flexibility to increase the coal flow rate to the hybrid gasifier to up to 1.2 kg/s from 1.0, when sufficient solar energy is available, reduces the magnitude of the dominant peak by 38% and thus the annually averaged utilization of the heliostat collection capacity from 67 to 76%. The flexibility to boost the fuel flow rate to the gasifier up to the intermediate value of 1.1 kg/s from 1.0 reduces by 20% the size of the dominant peak in the distribution and by 7% the annual average utilization of the heliostat field.

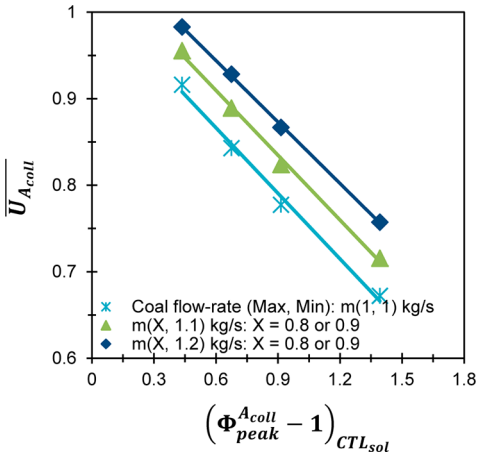

Figure 9. Dependence of the annually averaged utilization of the installed heliostat collection capacity on the normalized excess heliostat collection capacity for the CTL_{sol} polygeneration system and for three coal flow rate flexibility scenarios. The curves with different minimum limit on the coal flow rate are combined because this parameter was found not to effect the utilization of the heliostat field.

Figure 9 presents the dependence of the annually averaged utilization of the heliostat field ($\overline{U}_{A_{coll}}$) on the excess heliostat field area, $(\Phi_{peak}^{A_{coll}} - 1)_{CTL_{sol}}$. This shows that allowing a boost in the maximum coal flow rate to the gasifier of up to 1.2 kg/s, from 1 kg/s, increases $\overline{U}_{A_{coll}}$ by 6−13% for a given $\Phi_{peak}^{A_{coll}} - 1$ range. In comparison, an intermediate maximum coal flow rate of 1.1 kg/s leads to a 4−7% improvement in $\overline{U}_{A_{coll}}$ over the constant flow rate hybrid gasifier operational scenario.

Figure 10 also shows that the hybrid gasifier's annually averaged utilization, $\overline{U}_{HG}$ is fairly insensitive to $\Phi_{peak}^{A_{coll}} - 1$ but very sensitive to the fuel turn-down/boost operational scenario. Relative to the constant flow rate scenario, the $\overline{U}_{HG}$ is shown to fall by 12 percentage points for the $\dot{m}_{(1.1,0.9)}$ kg/s operational scenario and to fall by 24 percentage points for the $\dot{m}_{(1.2,0.8)}$ kg/s scenario. Interestingly, the $\dot{m}_{(1.2,0.9)}$ and $\dot{m}_{(1.1,0.9)}$ kg/s scenarios are estimated to both yield $\overline{U}_{HG} \sim 82\%$. Importantly, flexibly

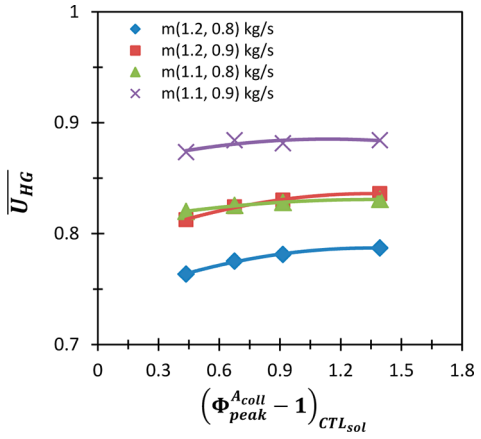

Figure 10. Dependence of the annually averaged utilization of the hybrid gasifier on the normalized excess heliostat collection capacity for the CTL_{sol} polygeneration system, for four coal flow operational flexibility scenarios.

boosting or turning down the flow rate has a larger influence on $\overline{U}_{HG}$ than does varying the heliostat collection area.

Taken together, Figures 9 and 10 highlight the inevitable trade-off between maximizing the economic utilization of the heliostat field and the hybrid solar gasifier. Maximizing the utilization of the heliostat field compromises the utilization of the hybrid gasifier, but this has the benefit of increasing the solar share of the process and thus the energetic and GHG emissions performance of the CTL_{sol} polygeneration system. Note that Figures 9 and 10 also assume that the dynamic variation in fuel flow to the reactor does not significantly influence either the scheduled or unscheduled plant maintenance. While yet to be confirmed, this assumption is considered to be reasonable because these turn-down/fuel-boost ratios are comparable with standard ratios of similar commercial gasification equipment.[43]

3.2. Hybrid Solar Coal Gasification Integrating Dry/Steam Natural Gas Reformer ($CTL_{sol,NG(dry/steam)}$). Figure 11 compares the effect of incorporating dry reforming or steam co-reforming of natural gas with the CTL_{sol} polygeneration system on the calculated mine-to-tank (MTT) CO_2-e emissions as a function of the normalized excess heliostat collection capacity $(\Phi_{peak}^{A_{coll}} - 1)_{CTL_{sol,(NG)}}$. It can be seen that both the $CTL_{sol,NG(dry)}$ and $CTL_{sol,NG(steam)}$ systems enable approximately the same reduction in emissions of ~15 ± 1.5 kg CO_2-e/GJ ($Q_{FTL} + W_{net}$) relative to the CTL_{sol} system. Relative to the autothermal CTL_{ref} system, this constitutes a 43−46% reduction in emissions, which corresponds to a further 12 percentage point reduction over that enabled by the CTL_{sol} system. Figure 11 also shows that there is little benefit to the GHG emissions from extending the excess heliostat collection capacity above 50%. Importantly, both $CTL_{sol,NG}$ systems examined produce ~32 kg CO_2-e/GJ ($Q_{FTL} + W_{net}$) more emissions than do the tar-sands-derived diesel, which is the most carbon intensive form of diesel currently in production.[5] That is, the use of solar energy alone, with 70−30% calorific fraction of coal to natural gas, in a hybrid gasification, co-reforming process, is not sufficient to achieve parity with conventional diesel production. Hence, additional approaches are required, such as blending with biomass.

Figure 12 presents the energetic performance of both the CTL_{sol} and $CTL_{sol,NG(dry)}$ and $CTL_{sol,NG(steam)}$ systems as a

dx.doi.org/10.1021/ef400217n | Energy Fuels 2013, 27, 3556−3569

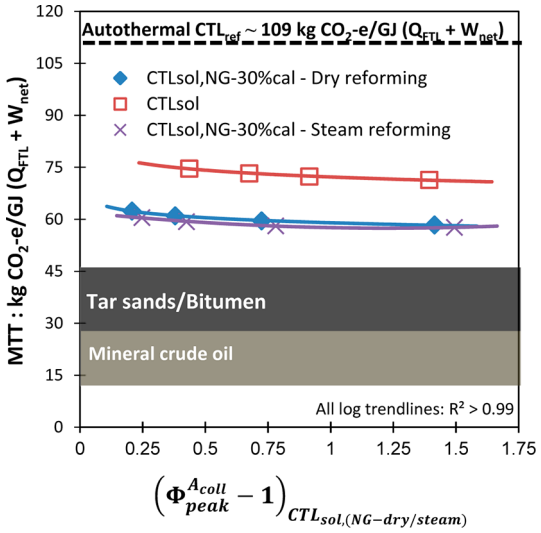

Figure 11. Dependence of mine-to-tank (MTT) CO_2-e emissions on the normalized heliostat collection area for the CTL_{sol} and $CTL_{sol,NG(dry)}$ and $CTL_{sol,NG(steam)}$ systems. Assumptions: coal gasification T_g = 1100 °C; $\dot{m}_{(1.2,0.8)}$ kg/s flexibility in coal flow; natural gas dry/steam internal reforming at 1050 °C, 11 bar-a, with no flexibility in NG flow in response to solar insolation.

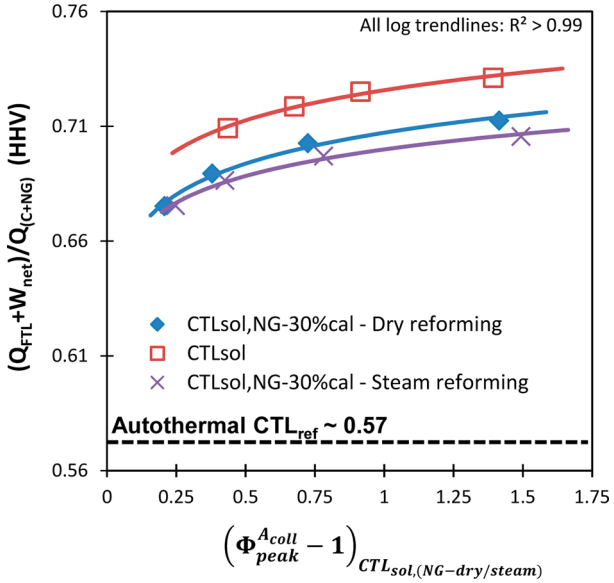

Figure 12. Dependence of total energetic productivity on the normalized heliostat collection area for the CTL_{sol} and $CTL_{sol,NG(dry)}$ and $CTL_{sol,NG(steam)}$ systems. Assumptions: coal gasification T_g = 1100 °C; $\dot{m}_{(1.2,0.8)}$ kg/s coal flow flexibility operational scenario; natural gas dry/steam internal reforming at 1050 °C, 11 bar-a, with no flexibility in NG flow in response to solar insolation.

function of $(\Phi_{peak}^{A_{coll}} - 1)_{CTL_{sol,(NG)}}$. This shows that the energetic productivity increases significantly with A_{coll} for all cases throughout the range. Interestingly, a small but significant reduction of 2 percentage points is estimated for the $CTL_{sol,NG(dry)}$ and $CTL_{sol,NG(steam)}$ systems, relative to the CTL_{sol} system for A_{coll} = 89 × 10^3 m^2 and a 5 percentage points reduction for A_{coll} = 44 × 10^3 m^2. Furthermore, the $CTL_{sol,NG(dry)}$ and $CTL_{sol,NG(steam)}$ systems enable, respectively, a 34 or 32% increase in the absolute energetic output relative to the CTL_{sol} configuration.

Figure 13 presents the relationship between the solar share of the CTL_{sol}, the $CTL_{sol,NG(dry)}$, and the $CTL_{sol,NG(steam)}$ systems' individual net energetic output as a function of $(\Phi_{peak}^{A_{coll}} - 1)_{CTL_{sol,(NG)}}$. It can be seen that the solar share of the output increases with the size of the normalized heliostat collection capacity for all scenarios, by approximately three percentage points from 19 to 22% for the CTL_{sol} system, 15 to 20% for the $CTL_{sol,NG(dry)}$, and 15 to 19% for the $CTL_{sol,NG(steam)}$ systems. This result shows that the integration of the natural gas co-reforming system decreases the solar share of the polygeneration system as the solar upgrade achieved by natural gas reforming is smaller than that achieved by coal gasification.

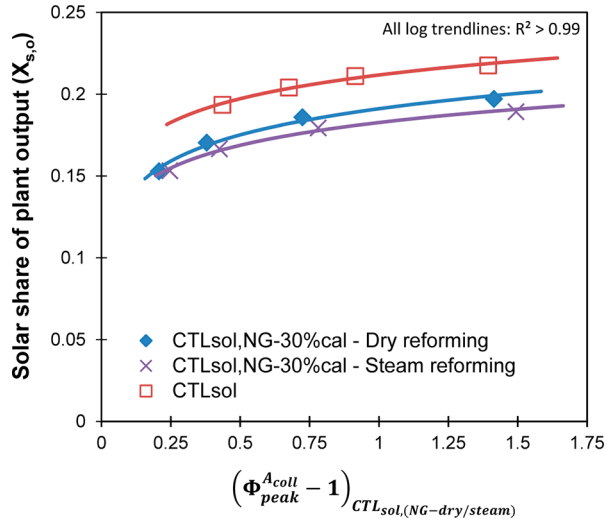

Figure 13. Dependence of the solar share of plant output ($X_{s,o}$) from Sheu et al.[6] on the normalized heliostat collection area for the CTL_{sol} and $CTL_{sol,NG(dry)}$ and $CTL_{sol,NG(steam)}$ systems. Assumptions: coal gasification T_g = 1100 °C; $\dot{m}_{(1.2,0.8)}$ kg/s coal flow flexibility operational scenario; natural gas dry/steam internal reforming at 1050 °C, 11 bar-a, with no flexibility in NG flow in response to solar insolation.

Nevertheless, given the low expected cost[13] of integrating a NG co-reforming system within an entrained flow autothermal gasifier, its integration within a hybrid solar gasifier could enable significant improvements to the economic productivity of the reactor assembly, heliostat collection field, and downstream unit operations. It should be clear, however, that this expectation of a low cost of integration is based on the balance-of-plant savings that are assumed to apply to the proposed solar integrated, $CTL_{sol,NG}$ polygeneration system as they do for the equivalent autothermal polygeneration system.[13] The $CTL_{sol,NG(dry)}$ system's annually averaged $\overline{U_{A_{coll}}}$ is estimated to be between 7 (A_{coll} = 44 × 10^3 m^2) and 13 (A_{coll} = 63 × 10^3 m^2) percentage points larger than the CTL_{sol}, assuming the $\dot{m}_{(1.1,0.9)}$ kg/s flexibility case (see Figure 11). This is an important result as the hybrid solar vortex gasifier[2,13,25−29] and heliostat field[30,39] are likely to be the most expensive components of a CTL_{sol} polygeneration facility.

Interestingly, while the addition of either dry or steam reforming to the solar-hybridized gasification process yields significant benefits that are broadly similar (Figure 12), there are some small differences. Unlike in Figure 11, where the emissions of the $CTL_{sol,NG(dry)}$ system converge to match those of the $CTL_{sol,NG(steam)}$ system as the excess collection capacity is increased, the energetic productivity of the two systems

dx.doi.org/10.1021/ef400217n | Energy Fuels 2013, 27, 3556−3569

diverges with increasing excess field capacity. This is a result of the $CTL_{sol,NG(dry)}$ system's larger total endothermic demand (see Table 2), which enables it to consume more of the solar energy that becomes available as the excess heliostat collection capacity is increased. However, the $CTL_{sol,NG(dry)}$ system's larger energetic productivity is balanced by the low H_2/CO ratio of the raw syngas output from the co-reformer, leading to its WGS upgrading process producing 3% more CO_2-e emissions than the $CTL_{sol,NG(steam)}$ WGS process. This leads to the two systems having approximately the same CO_2-e emissions profile in Figure 11.

3.3. Hybrid Solar Coal-Biomass to Liquids ($CTL_{sol,bio}$) System. Figure 14 presents the mine-to-tank (MTT) CO_2-e emissions from the $CTL_{sol,bio}$ system as a function of the biomass fuel weight fraction (m_B/m_{C+B}). Also shown is a comparison of the $CTL_{sol,bio}$ system's CO_2-e emissions performance with that of the nonsolar, autothermal CTL_{bio} polygeneration system. The calculated MTT CO_2-e emissions of the $CTL_{sol,bio}$ system were credited with the proportion of biomass, on a carbon mol fraction basis, combusted at the point of end-use. Figure 14 shows that the $CTL_{sol,bio}$ system achieves CO_2-e emissions parity with the upper limit of conventional diesel from tar sands for $m_B/m_{C+B} \sim 0.3$.[5] In comparison, emissions from the nonsolar CTL_{bio} system are calculated to match those of diesel derived from tar sands for $m_B/m_{C+B} \sim 0.45$.[5] For $m_B/m_{C+B} \sim 0.53$, the $CTL_{sol,bio}$ system's energetic output achieves lower GHG emissions than all forms of mineral crude currently in production.[4] Additionally, the $CTL_{sol,bio}$ system's MTT emissions are reduced to 0 for a biomass cogasification weight fraction of 60%, while the comparable autothermal CTL_{bio} system requires a biomass cogasification weight fraction of 70%. Furthermore, the CO_2-e emissions avoidance potential of the solar biomass-to-liquids, BTL_{sol} ($m_B/m_{C+B} = 1$) system is 13% higher on a MTT basis, than the nonsolar, autothermal CTL_{bio} polygeneration system, after accounting for the molar proportion of biomass-derived carbon burnt at the point of end-use. As expected, the percentage contribution of solar energy to the reduction in CO_2 emissions decreases with increasing m_B/m_{C+B} because the calorific content of coal is 1.36 times that of biomass on a mass basis. The potential for the solar-hybridized cogasification process to significantly reduce the amount of biomass required to meet a given CO_2-e emissions standard is important given biomass is typically three to four times more expensive than coal.

Figure 15 presents the total energetic productivity of the $CTL_{sol,bio}$ and the nonsolar, autothermal CTL_{bio} cases, as a function of the biomass fuel weight fraction (m_B/m_{C+B}). Here, the difference between the dotted and solid lines shows that the solar hybridization of the coal-biomass cogasification process increases by 27−33% the $CTL_{sol,bio}$ system's total specific energetic productivity over the range of biomass weight fractions from 0 to 100%. It is interesting to note that the BTL_{sol} system can yield 104% of the autothermal CTL_{ref} system's energetic productivity, whereas the autothermal, nonsolar BTL system yields only 72% of the autothermal CTL_{ref} system's energetic productivity. The improved energetic productivity of the solar-hybridized cogasification process is expected to significantly improve the viability of producing biofuels relative to the nonsolar autothermal process, especially because the cost of biomass is typically three to four times higher than that of coal.[34−36]

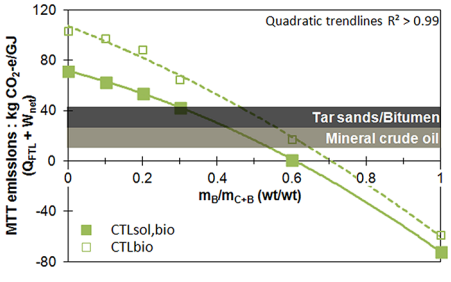

Figure 14. Dependence of the mine-to-tank (MTT) CO_2-e emissions of the $CTL_{sol,bio}$ system and the nonsolar, autothermal CTL_{bio} polygeneration system on the biomass blend fraction by weight (m_B/m_{C+B}). Assumptions: coal-biomass cogasification at T_g = 1100 °C; $\dot{m}_{(1.2,0.8)}$ kg/s flexibility in the blended fuel flow to gasifier; A_{coll} = 63 × 10^3 m^2.

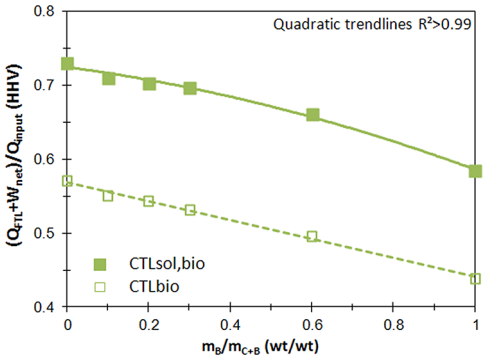

Figure 15. Dependence of the total specific energetic productivity of the $CTL_{sol,bio}$ system and the nonsolar, autothermal CTL_{bio} polygeneration facility on the biomass blend fraction by weight (m_B/m_{C+B}). Assumptions: coal-biomass cogasification at T_g = 1100 °C, P_g = 1 bar-a; $\dot{m}_{(1.2,0.8)}$ kg/s flexibility in the blended fuel flow to gasifier; A_{coll} = 63 × 10^3 m^2.

3.4. Steam Consumption. Figure 16 presents the annually averaged consumption of steam by the hybrid gasifier for the reference hybrid solar gasifier in comparison with three other cases. It can be seen that the CTL_{sol} system consumes ∼2% more steam than the CTL_{ref} system, while the $CTL_{sol,bio\text{-}60wt\%}$ process consumes 20% less. The $CTL_{sol,NG(dry)}$ system has the highest specific rate of steam consumption, which is an additional 7% per mole of SG_{up} than the CTL_{ref} system. In comparison with the dry reforming integrated process, the $CTL_{sol,NG(steam)}$ consumes 10% less steam than the CTL_{ref} system.

Interestingly, Figure 16 also shows that over 74% of the $CTL_{sol,NG(steam)}$ system's total steam consumption can be attributed to co-reformer section of the hybrid gasifier, whereas it is ∼31% for the $CTL_{sol,NG(dry)}$ configuration. The balance of the steam for both processes is consumed in the water−gas shift reactor, WGSR. The proportion of steam consumed by the solar-intensive hybrid gasification/co-reforming relative to the WGSR is an important issue as the most productive solar resources are often in arid regions where access to fresh water is difficult. One advantage of the $CTL_{sol,NG(dry)}$ process is that the gasifier section requires a proportionally low level of steam consumption relative to all other configurations (other than the 60 wt % biomass cogasification configuration). This advantage enables the option to separate the solar energy intensive gasification/dry co-reforming process' from the water-intensive downstream processes to a site where water availability is less constrained.

dx.doi.org/10.1021/ef400217n | Energy Fuels 2013, 27, 3556−3569

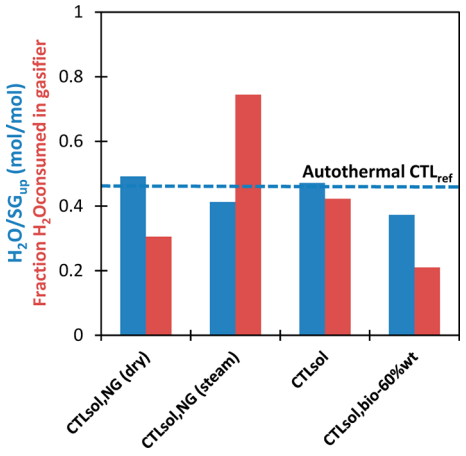

Figure 16. Annually averaged ratio of the total molar steam consumption to the production of upgraded syngas ($SG_{up}/H_2/CO \sim 2.26$) (blue); annually averaged fraction of steam consumed by the hybrid gasifier relative to the total (red) for four CTL_{sol} plant scenarios and the CTL_{ref} system.

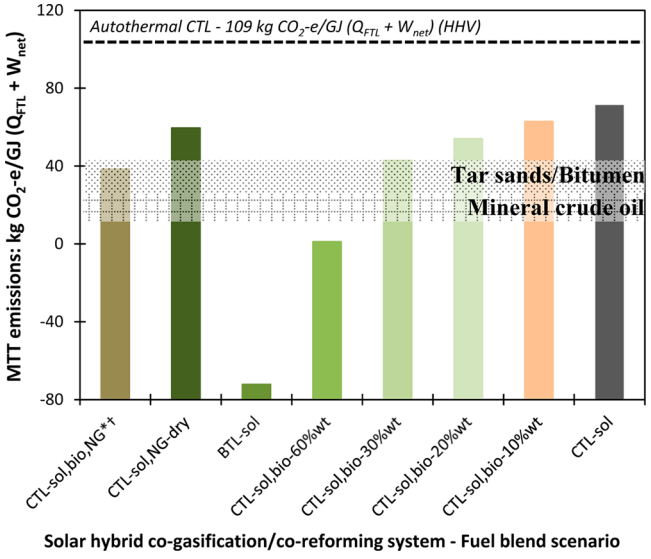

Figure 17. Summary of the mine-to-tank (MTT) CO_2-e emissions performance of the CTL_{sol} base system for all range of fuel blend scenarios (*m_B/m_{C+B} = 30 wt %, †Q_{NG}/Q_{total} = 30% cal). All scenarios are based on the $\dot{m}_{(1.2,0.8)}$ kg/s operational flexibility scenario in solid (biomass-coal blend) fuel flow, $A_{coll} = 63 \times 10^3$ m^2, T_g = 1100 °C, and P_g = 1 bar-a.

3.5. Overall Scenario Comparison. Figures 17 and 18 summarize the MTT CO_2-e emissions and total energetic productivity (HHV) for eight key scenarios of fuel blends and hybrid solar gasification reactor configurations. In particular, Figure 17 shows that the use of solar gasification with a 30% blend of biomass (the $CTL_{sol,bio\text{-}30wt\%}$ case) achieves CO_2-e emissions parity with that of conventional production of synthetic crude from tar sands, while the further incorporation of a natural gas dry co-reformer as part of the $CTL_{sol,bio\text{-}30\%wt,NG}$ system achieves an additional 10% reduction in MTT emissions. On a mine-to-tank basis, the $CTL_{sol,bio\text{-}60wt\%}$ system produces 0 CO_2-e emissions and the solar gasification with pure biomass enables a net avoidance of 72 kg CO_2-e/GJ (Q_{FTL} + W_{net}) on a MTT basis. It is important to note that these CO_2-e emissions results are credited with the molar proportion of biomass that is burnt at the point of end-use.

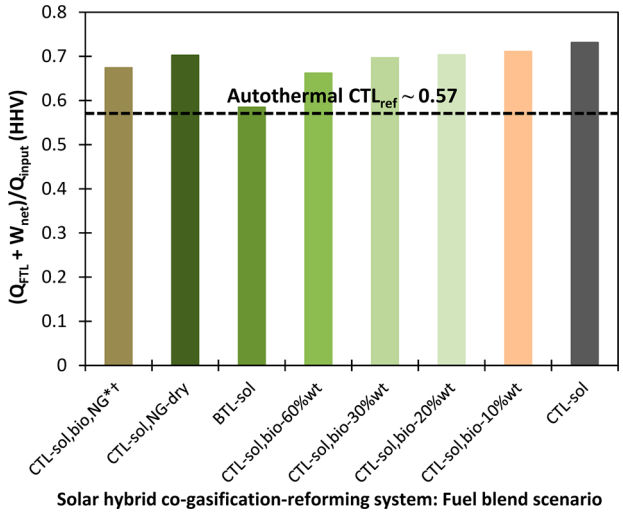

Figure 18. Summary of the total energetic productivity of the CTL_{sol} base system for a range of fuel blend scenarios (*m_B/m_{C+B} = 30 wt %, †Q_{NG}/Q_{total} = 30% cal). All scenarios are based on the $\dot{m}_{(1.2,0.8)}$ kg/s operational flexibility scenario in solid (biomass-coal blend) fuel flow, $A_{coll} = 63 \times 10^3$ m^2, T_g = 1100 °C, and P_g = 1 bar-a.

Figure 18 shows the $CTL_{sol,bio,NG}$ system to have 95% of the energetic productivity of the $CTL_{sol,bio\text{-}30wt\%}$, but this corresponds to a 37% improvement on an absolute energy output basis. This has important implications for the economic productivity of the hybrid cogasification reactor system. On the far right of the two distributions, the $CTL_{sol,NG}$ system has 94% of the carbon emissions of the $CTL_{sol,bio\text{-}10wt\%}$ configuration but energetic productivity that is only 2% lower.

It is worth noting that all of the results presented in Figures 17 and 18 are based on the $\dot{m}_{(1.2,0.8)}$ kg/s operational flexibility scenario in solid fuel flow to the gasifier. The sensitivity to variations in pressure and heliostat area is likely to be similar to the analysis presented in section 3.1.2 .

4. CONCLUSIONS

The incorporation of concentrated solar radiation into a coal-to-liquids, coal-natural-gas-to-liquids process or into a coal-biomass-to-liquids process offers significant potential advantages both to the energetic productivity of the polygeneration system and to lowering its mine-to-tank CO_2-e emissions intensity. In particular, solar hybridization decreases by up to 33% the weight fraction of biomass required to meet the CO_2-e emissions associated with diesel derived from tar sands and reduce by 17% the weight fraction required to eliminate CO_2-e emissions at production altogether relative to the autothermal cogasification-based, coal-biomass-to-liquids process. This may enable a significant economic advantage given that biomass has typically been 3−4 times more expensive than coal.[31,34−36]

The incorporation of an indirectly irradiated solar hybrid steam natural gas reformer within the hybrid gasifier ($CTL_{sol,NG}$) was shown to improve by 33% the system's absolute energetic output, reduce by 15% its GHG emissions, and improve by 15% the annually averaged utilization of a heliostat field with $A_{coll} = 63 \times 10^3$ m^2, relative to the CTL_{sol} system. Importantly, the dry co-reformer was found to halve the combined hybrid gasifier/co-reformer assembly's rate of water consumption relative to the steam co-reformer, while achieving

dx.doi.org/10.1021/ef400217n | Energy Fuels 2013, 27, 3556−3569

similar levels of improvement to the polygeneration system's energetic and environmental performance. Although, the low water consumption intensity of the hybrid gasifier/dry co-reformer is balanced by the higher consumption of water by the process' water-gas shift reactor relative to the system incorporating a steam co-reformer this is still an important result. Given the generally poor availability of fresh water in arid regions where the solar resource is most productive, the dry co-reforming process is a feasible path to reducing the steam consumption of the solar intensive section of the $CTL_{sol,NG}$ polygeneration process.

It is further found that both the energetic productivity and greenhouse gas mitigation could be improved by 4% and capital utilization of the heliostat array by up to 13% for $A_{coll} = 63 \times 10^3$ m^2 if the fuel feed rate to the hybrid gasifier could be varied flexibly by ±20% relative to the nominal design value of 1 kg/s in response to transient fluctuations in solar input. Interestingly, the present assessment also found that the overall energetic performance of the hybrid system is only weakly sensitive to gasifier operating pressure. This is because the FTL liquid heating value forms >85% of the net energy output. This is significant, as operation of a solar gasifier at atmospheric pressure increases the viability of using direct solar radiation heat transfer, notably by increasing the feasibility of a window or aperture through which the solar radiation can be introduced into the reactor.

AUTHOR INFORMATION

Corresponding Author

*E-mail: ashok.kaniyal@adelaide.edu.au. Phone: +61403691321.

Notes

The authors declare no competing financial interest.

ACKNOWLEDGMENTS

A.A.K. would like to thank the generous support of Ricoh for providing the Clean Energy Scholarship. P.J.vE. would like to acknowledge the support of the Australian Solar Institute (ASI) for providing a postdoctoral fellowship. The Australian Government, through the ASI, is supporting Australian research and development in solar photovoltaic and solar thermal technologies to help solar power become cost competitive with other energy sources. G.J.N. wishes to thank the Australian Research Council (ARC) for the Discovery Outstanding Researcher Award in the thermal applications of concentrated solar radiation. The authors gratefully acknowledge the financial and other support received for this research from the Energy Pipelines Cooperative Research Centre (EPCRC) which was established under the Australian Government's Cooperative Research Centre's program.

NOMENCLATURE

A_{coll} – heliostat field area (m^2)
AR – as received
BTL – biomass to liquids polygeneration system
cal – calorific fraction (%)
CCS – carbon capture and storage technology
CTL – coal to liquids polygeneration system
d.a.f. – dry, ash-free basis
FT – Fischer−Tropsch reactor
FTL – Fischer−Tropsch liquid fuels
GHG – greenhouse gas
$\dot{m}$ or m – fuel mass flow rate (kg/s) or fuel mass (kg)
mol – molar fraction
MTT – mine-to-tank CO_2-e emissions
NGR – natural gas reformer
$\dot{Q}$ or Q – thermal power or heat
$\overline{U}$ – average capital utilization
$\dot{W}$ or W – power or work output
wt – weight (%)
$\dot{m}_Y$ – flow rate of fuel "Y" in kg/s; where Y can be coal, natural gas, or a coal-biomass blend
HHV – higher heating value

Greek letters

Φ – ratio of the net solar thermal power output from the heliostat array($\dot{Q}_{sol,net}$) to the total endothermic demand of completely gasifying the fuel fed into the hybrid gasifier and co-reformer (if applicable) at an assumed reactor temperature ($\dot{Q}_{HG,(NRG)}^{T_g\text{-}R}$)
η – efficiency
$\Phi_{peak}^{A_{coll}} - 1$ – fraction by which the annual peak net solar thermal power output of the heliostat array exceeds the gasifier's total endothermic demand

Superscripts

ann. peak – peak hourly averaged value from a year-long time series
NGR – refers to thermal power required by the natural gas (dry/steam) reformer to completely convert $\dot{m}_{NG}$ kg/s of fuel to raw syngas
T_g-R – temperature at which gasification reactions occur

Subscripts

abs – solar energy absorption efficiency
ann – parameter based on year-long time series
B – biomass fuel
bio-Xwt% – cogasification of X wt% biomass with coal
C+B – coal + biomass fuel blend
C – coal fuel
dry – CO_2 natural gas reforming
FTL – Fischer−Tropsch liquids
HG – hybrid, entrained flow solar gasifier
isen – isentropic efficiency of compressors/turbines
(min,max) – the minimum and maximum values of an operating range
net – net (of parasitic losses) electrical output or flow of thermal power from the heliostat field to the solar hybrid reactor (net of optical and reradiation losses)
NG – natural gas fuel
opt – heliostat field optical efficiency
R – thermal power required to enable conversion of 99% of design coal at a fuel flow rate of 1 kg/s
raw – syngas output straight from the gasifier
ref – autothermal, reference CTL polygeneration system
sol – solar
steam – steam natural gas reforming
stg – refers to stored levels of O_2 and SG_{up}
total – calorific value of total fuel input to the solar hybrid cogasification, co-reforming reactor
up – upgraded syngas output from the sweet WGSR (H_2/CO = 2.26:1)

wall – heat losses through the walls of the entrained flow gasifier

REFERENCES

(1) Takeshita, T.; Yamaji, K. Important roles of Fischer−Tropsch synfuels in the global energy future. *Energy Policy* **2008**, *36*, 2773−2784.

(2) Liu, G.; Larson, E.; Williams, R.; Kreutz, T.; Guo, X. Making Fischer−Tropsch fuels and electricity from coal and biomass: performance and cost analysis. *Energy Fuels* **2011**, *25*, 415−437.

(3) Meerman, J.; Ramirez, A.; Turkenburg, W.; Faaij, A. Performance of simulated flexible integrated gasification polygeneration facilities. Part A: A technical-energetic assessment. *Renew. Sustain. Energy Rev.* **2011**, *15*, 2563−2587.

(4) Gerdes, K.; Skone, T. J. *An Evaluation of the Extraction, Transport and Refining of Imported Crude Oils and the Impact on Life Cycle Greenhouse Gas Emissions*; NETL: Pittsburgh, PA, 2009; p 42.

(5) Lattanzio, R. *Canadian Oil Sands: Life-Cycle Assessments of Greenhouse Gas Emissions*; Congressional Research Service: Washington DC, 2012; p 31.

(6) Sheu, E.; Mitsos, A.; Eter, A.; Mokheimer, E.; Habib, M.; Al-Qutub, A. A review of hybrid solar-fossil fuel power generation systems and performance metrics. *J. Solar Energy Eng.* **2012**, 134.

(7) Kribus, A.; Zaibel, R.; Carey, D.; Segal, A.; Karni, J. A solar-driven combined cycle power plant. *Sol. Energy* **1998**, *62*, 121−129.

(8) Ordorica-Garcia, G.; Delgado, A.; Garcia, A. Novel integration options of concentrating solar thermal technology with fossil-fuelled and CO_2 capture processes. *Energy Procedia* **2011**, *4*, 809−816.

(9) Nathan, G.; Battye, D.; Ashman, P. Economic evaluation of a novel fuel-saver hybrid combining a solar receiver with a combustor for a solar power tower. *Appl. Energy* **2012**, submitted for review.

(10) Kaniyal, A.; van Eyk, P.; Nathan, G.; Ashman, P.; Pincus, J. Polygeneration of liquid fuels and electricity by the atmospheric pressure hybrid solar gasification of coal. *Energy Fuels* **2013**, submitted for review.

(11) Turchi, C.; Ma, Z.; Erbes, M. Gas turbine/solar parabolic trough hybrid designs. In *ASME Turbo Expo 2011*, NREL: Vancouver, Canada, 2011.

(12) Sudiro, M.; Bertucco, A. Synthetic fuels by a limited CO_2 emission process which uses both fossil and solar energy. *Energy Fuels* **2007**, *21*, 3668−3675.

(13) Adams, T., II; Barton, P. Combining coal gasification and natural gas reforming for efficient polygeneration. *Fuel Process. Technol.* **2011**, *92*, 639−655.

(14) Dahl, J.; Weimer, A.; Lewandowski, A.; Bingham, C.; Bruetsch, F.; Steinfeld, A. Dry reforming of methane using a solar-thermal aerosol flow reactor. *Ind. Eng. Chem. Res.* **2004**, *43*, 5489−5495.

(15) Weimer, A. Solar thermal chemical processing challenges and commercial path forward. *Curr. Opin. Chem. Eng.* **2012**, *1*, 211−217.

(16) Trainham, J.; Newman, J.; Bonino, C.; Hoertz, P.; Akunuri, N. Whither solar fuels? *Curr. Opin. Chem. Eng.* **2012**, *1*, 204−210.

(17) Steinfeld, A.; Palumbo, R. Solar thermochemical process technology. In *Encyclopedia of Physical Science & Technology*; Meyers, R., Ed.; Academic Press: New York, 2001; Vol. *15*, pp 237−256.

(18) Opoku-Gyamfi, K.; Adesina, A. Forced composition cycling of a novel thermally self-sustaining fluidised-bed reactor for methane reforming. *Chem. Eng. Sci.* **1999**, *54*, 2575−2583.

(19) ABARES, Australian Energy Resource Assessment. In *ABARES*; Australian Government: Canberra, 2010.

(20) Sun, Y.; Ritchie, T.; Hla, S.; McEvoy, S.; Stein, W.; Edwards, J. Thermodynamic analysis of mixed and dry reforming of methane for solar thermal applications. *J. Nat. Gas Chem.* **2011**, *20*, 568−576.

(21) Price, L. Origins, characteristics, controls and economic viabilities of deep-basin gas resources. *Chem. Geol.* **1995**, *126*, 335−349.

(22) Z'Graggen, A.; Haueter, P.; Maag, G.; Romero, M.; Steinfeld, A. Hydrogen production by steam-gasification of carbonaceous materials using concentrated solar power - IV. Reactor experimentation with vacuum residue. *Int. J. Hydrogen Energy* **2008**, *33*, 679−684.

(23) Z'Graggen, A.; Haueter, P.; Maag, G.; Vidal, A.; Romero, M.; Steinfeld, A. Hydrogen production by steam-gasification of petroleum coke using concentrated solar power - III. Reactor experimentation with slurry feeding. *Int. J. Hydrogen Energy* **2007**, *32*, 992−996.

(24) Z'Graggen, A.; Steinfeld, A. Hydrogen production by steam-gasification of carbonaceous materials using concentrated solar energy - V. Reactor modeling, optimization and scale-up. *Int. J. Hydrogen Energy* **2008**, *33*, 5484−5492.

(25) Kreutz, T.; Larson, E.; Liu, G.; Williams, R. In *Fischer−Tropsch Fuels from Coal and Biomass*, 25th Ann. Intl Pittsburgh Coal Conference; Pittsburgh, Pennsylvania, 2008.

(26) Kreutz, T.; Williams, R.; Consonni, S.; Chiesa, P. Co-production of hydrogen, electricity and CO_2 from coal with commercially ready technology. Part B: Economic analysis. *Int. J. Hydrogen Energy* **2005**, *30*, 769−784.

(27) Larson, E.; Fiorese, G.; Liu, G.; Williams, R.; Kreutz, T.; Consonni, S. Co-production of decarbonized synfuels and electricity from coal + biomass with CO_2 capture and storage: An Illinois case study. *Energy Environ. Sci.* **2010**, *3*, 28−42.

(28) Meerman, J.; Ramirez, A.; Turkenburg, W.; Faaij, A. Performance of simulated flexible integrated gasification polygeneration facilities, Part B: Economic evaluation. *Renew. Sustain. Energy Rev.* **2012**, *16*, 6083−6102.

(29) Woods, M.; Capicotto, P.; Haslbeck, J.; Kuehn, N.; Matuszewski, M.; Pinkerton, L.; Rutkowski, M.; Schoff, R.; Vaysman, V. *Bituminous Coal and Natural Gas to Electricity Final Report*, DoE/NETL-2007/1281; US DoE, August 2007; Vol. *1*.

(30) Kolb, G.; Jones, S.; Donnelly, M.; Gorman, D.; Thomas, R.; Davenport, R.; Lumia, R. *Heliostat Cost Reduction Study*; Sandia National Laboratories: Alburquerque, NM, 2007; p 158.

(31) Berndes, G.; Hoogwijk, M.; van den Broek, R. The contribution of biomass in the future global energy supply: a review of 17 studies. *Biomass Bioenergy* **2003**, *25*, 1−28.

(32) Baxter, L. Biomass-coal co-combustion: opportunity for affordable renewable energy. *Fuel* **2005**, *84*, 1295−1302.

(33) Kirkels, A.; Verbong, G. Biomass gasification: Still promising? A 30-year global overview. *Renew. Sustain. Energy Rev.* **2011**, *15*, 471−481.

(34) Sami, M.; Annamalai, K.; Woolridge, M. Co-firing of coal and biomass fuel blends. *Prog. Energy Combust. Sci.* **2001**, *27*, 171−214.

(35) De, S.; Assadi, M. Impact of cofiring biomass with coal in power plants—A techno-economic assessment. *Biomass Bioenergy* **2009**, *33*, 283−293.

(36) Tijmensen, M.; Faaij, A.; Hamelinck, C.; van Hardeveld, M. Exploration of the possibilities for production of Fischer−Tropsch liquids and power via biomass gasification. *Biomass Bioenergy* **2002**, *23*, 129−152.

(37) NREL *National Solar Radiation Database Update: User'S Manual*, 1991−2005 update; US DoE; Golden, CO, 2007.

(38) NREL National solar radiation database 1991−2005 update.

(39) Meier, A.; Gremaud, N.; Steinfeld, A. Economic evaluation of the industrial solar production of lime. *Energy Convers. Manage.* **2005**, *46*, 905−926.

(40) Higman, C.; van der Burgt, M. *Gasification*, 2nd ed.; Elsevier: Oxford, UK, 2008.

(41) Melchior, T.; Perkins, P.; Lichty, A.; Weimer, A.; Steinfeld, A. Solar-driven biochar gasification in a particle-flow reactor. *Chem. Eng. Proc.* **2009**, *48*, 1279−1287.

(42) Moghtaderi, B.; Sheng, C.; Wall, T. An overview of the Australian biomass resources and utilization technologies. *BioResources* **2006**, *1*, 93−115.

(43) Marbe, Å.; Harvey, S.; Berntsson, T. Biofuel gasification combined heat and power—new implementation opportunities resulting from combined supply of process steam and district heating. *Energy* **2004**, *29*, 1117−1137.